Soft Matter

PAPER

View Article Online
View Journal | View Issue

Cite this: *Soft Matter*, 2025, **21**, 3304

Microfiber suspensions for the removal of adhered colloids from surfaces, microdevices, and cavities

Marcel M. Louis, [a] Samantha A. McBride, [b] Janine K. Nunes, [a] Antonio Perazzo, [c] Christopher A. Kuchar, [c] Mohamed E. Labib [c] and Howard A. Stone *[a]

Received 19th January 2025,
Accepted 19th March 2025

DOI: 10.1039/d5sm00065c

rsc.li/soft-matter-journal

Effective methods for cleaning surfaces are important for applications including dentistry, healthcare, micro-devices, and the manufacturing of electronic components and semiconductors. For example, surgical and dental instruments are susceptible to accumulation of aggregates and biofilm formation, which can lead to cross-contamination when ineffectively cleaned and reused. Complex fluids such as micro-fibrillated cellulose (MFC) can greatly assist in mechanically cleaning surfaces by removing strongly adhered aggregates without abrading the underlying material. We demonstrate that the heterogeneous structure of micro-fibrillated cellulose is effective in removing adhered particulates from surfaces and we characterize the cleaning efficiency of MFC suspensions in representative flow configurations. The experiments reported here involve flowing MFC solutions at various concentrations and at controlled shear rates through a rectangular microfluidic channel. Fluorescence microscopy is used to measure the removal of fluorescent particles that are adhered to the glass surface of the microfluidic device by electrostatic and surface forces. The particle removal with time is analyzed for each concentration of the MFC suspension and each shear rate to determine cleaning effectiveness. The rheology of the MFC solutions is also characterized and correlated to cleaning performance. We find that cleaning effectiveness increases with increasing fiber concentration and with increasing shear rate. Additionally, we compared the cleaning performance of the MFC suspensions with fluids that share similar rheological properties to highlight the role of shear thinning, elasticity, and tribology. Finally, we examine how sharp corners/edges within a microfluidic channel hinder cleaning and identify strategies for mitigating this hindrance.

1 Introduction

The detachment of adhered colloids from solid substrates is ubiquitous in many health, environmental, and technological applications.[1–3] In healthcare, the possibility of cross-contamination due to biofouling, and other colloidal materials, on reusable medical instruments poses potential health risks,[4] particularly to immunocompromised patients. For example, endoscopes are often contaminated with leftover bacteria after gastroscopy and colonoscopy procedures cause infection in vulnerable patients.[5,6] In skin care, there is a need for more innovative methods to remove biofilms/debris without irritating the surface of the skin.[7–9] Similarly, in oral hygiene, there is a need for more effective methods to remove adhered aggregates such as plaque, which is caused by a build-up of microorganisms. Traditional techniques for plaque removal involve abrasive brushing, which can be harsh on gums and is also ineffective at removing aggregates trapped between teeth.[10,11]

Gentle but effective cleaning methods that are not abrasive are also important in technological applications including the manufacture of electronics and semiconductors.[12,13] For example, precision cleaning for electronics is crucial for removing flux residues and particles from circuit boards and other electronic components. A large percentage of the produced integrated circuits go to waste due to contamination by micro-particles, which presents a significant environmental concern.[12] Similarly, the semiconductor industry requires ultra-clean surfaces for chip fabrication.[13–15] A gentle and surfactant-free cleaning solution could prevent the scratching of wafer surfaces and the deposition of surfactant residues that affect chip performance.

Past strategies for cleaning often rely on external forces such as scrubbing to physically detach particles from substrates.[16,17] Chemical etching can also be used to remove adhered contaminants.[18] While effective for planar surfaces, these methods must balance cleaning efficacy with substrate integrity.[17] In addition, mechanical strategies tend to be limited in their ability to remove

[a] *Department of Mechanical and Aerospace Engineering, Princeton University, Princeton, NJ, USA. E-mail: hastone@princeton.edu*
[b] *Department of Mechanical Engineering, University of Pennsylvania, Philadelphia, PA, USA*
[c] *NovaFlux, Princeton, NJ, USA*

adhered colloid particles from surfaces in confined geometries, such as micro-grooves, cavities, or channels or in the interstitial spaces between teeth.[3]

We can also mention green alternatives for cleaning ancient paper artifacts. Among the various surface cleaning methods for delicate materials such as paper, ancient artifacts, and paintings, nanostructured fluids and hydrogels are notable options.[19–21] However, their cleaning mechanism primarily relies on the solubilization, osmosis or wetting-induced detachment and capture of solid deposits rather than complex fluid flow-induced processes.

New strategies for preventing or reducing fouling in microfluidic devices are required to enable their reuse in applications including biomedical research, chemical analysis, and environmental monitoring.[22,23] These devices may feature small channels, edges, corners, contractions, and other surface structures that can trap particles, microbes, or other residues from prior uses or processing steps.[3,24] Particulate adhesion in microfluidic devices can also interfere with experimental measurements, for example, when fluorescent particles get trapped during particle image velocimetry (PIV).[3,25] Moreover, many microfluidic devices for research applications are single-use and generate non-recyclable plastic waste.[26] Thus, the ability to remove contaminants without damaging the device structure or altering the surface properties could improve the sustainable use of devices for microfluidic research. However, the complex geometries and confined spaces of micro-devices make them challenging to clean using traditional methods.[3] The development of effective cleaning protocols could improve the reliability, repeatability, and longevity of these devices.

One strategy that can be leveraged for colloidal detachment in smaller geometries, where surface tension forces can overcome particle–substrate adhesion, is to use air–liquid interfaces and the flow of air bubbles.[27–32] An important limitation to this method is that the moving air–liquid interfaces may not intersect with all colloids, particularly near corners in microdevices. Thus, many particles will be left behind in the corners once a bubble flows past. This poses a challenge for preventing bacterial contamination and biofilm regrowth, as remaining bacteria in the corners can quickly re-grow into the cleaned spaces. Moreover, microbubbles have been utilized to fracture the biofilms' extracellular matrix, leading to its removal and delayed regrowth in certain configurations.[33,34] Other strategies relying on fluid flow for *in situ* colloidal displacement include waves,[35] shearing flows,[36] and air jets.[37] Also, recent work has explored polymeric elastic stresses as a non-invasive and environmentally friendly approach to colloidal detachment, demonstrating promising results for free surfaces. For example, in Walker *et al.*,[38] a viscoelastic polyacrylamide (PAM) solution was used in cycles of jetting and siphoning flows to remove particles from a planar substrate, with the finding that higher concentrations of PAM increased particulate removal. We note that to the best of knowledge the use of complex fluids for *in situ* cleaning of microfluidic configurations has not been explored widely. A selection of work over the past 30 years exploring fluid flow strategies for detachment of colloidal particles from surfaces is shown in Table 1.

Here, we explore the use of a microfibrillated cellulose (MFC) in water suspension (produced by NovaFlux, Inc.) as a cleaning agent for the detachment of colloidal particles under a shearing flow in a microfluidic channel.[41] In contrast to the aforementioned methods that involve the use of chemical treatment or highly abrasive materials,[42] the use of MFC is purely mechanical without abrading or causing any other changes to surface properties. In fact, recent work has demonstrated that these MFC solutions containing entrapped silica particles can successfully remove both dental stains and dental plaque with limited abrasion to enamel surfaces.[43,44] MFC is a naturally derived material made from cellulose fibers. To create MFCs, cellulose fibers are stripped of their outer coatings to reveal individual fibrous bundles.[45] The fibrous nature of MFCs allows them to interact with particles adhered to surfaces and thereby facilitate detachment under shear. Because MFCs can be derived from plants and will degrade under natural conditions, these materials also present an environmentally sustainable and non-toxic cleaning solution. We demonstrate that MFC suspensions can be used to effectively remove particulate contamination from the interior of microfluidic devices, including corners, which are representative of small-scale confined geometries. Further, we explore the influence of both shear rate and MFC concentration on removal efficiency within both the center of the channel and from the corners.

2 Experiments

2.1 Cleaning fluid

We report the results of particle and aggregate removal by a micro-fibrillated cellulose-water suspension. The raw material,

Table 1 Chronological selection of previous experimental and theoretical works and the respective approach to the detachment of different types of colloids from different substrate configurations

Year	Authors	Geometry	Method of detachment	Colloid type
1993	Busnaina *et al.*[14]	Free surface	Hydrodynamic drag	Polystyrene latex
1995	Yiantsios *et al.*[39]	Parallel plates	Shear flow	Spherical glass
1997	Noordmans *et al.*[40]	Parallel plates	Bubble driven	Polystyrene latex
2000	Gomez-Suarez *et al.*[27]	Rectangular channel	Bubble driven	Polystyrene latex
2009	Kim *et al.*[35]	Free surface	Megasonic waves	Polystyrene latex
2006	Hirano *et al.*[37]	Free Surface	Nitrogen jet	Nitride
2011	Andreev *et al.*[36]	Free surface	Multi-phase shear flow	Silicon nitride
2014	Walker *et al.*[38]	Free surface	Elastic flows	Silica
2017	Khodaparast *et al.*[28]	Rectangular channel	Bubble driven	*Staphylococcus Aureus*

MFC, is supplied by Borregaard (Norway) under the trade name "Exilva Forte." NovaFlux produces the suspension in water, achieved through high-shear mixing to disperse the fibers. To observe the microstructure of the MFC suspension, we fluorescently labeled the microfibrillated cellulose with dichlorotrianzinyl–aminofluorescein using established labeling procedures.[46] The resulting structure of the MFC suspension was imaged under the microscope and is shown in Fig. 1, where we can observe that the form of the fibers is heterogeneous in nature, with elongated shapes and thicknesses that vary. The typical size of the fibers range from nanometers to hundreds of micrometers. In Fig. 1(b) we note that the green represents fiber-rich regions whereas the black represents the surrounding solvent (water). From this, we see that in solution the fibers form a fibrillar entangled network. Later, we will show how this network impacts rheology and cleaning effectiveness.

In this study, we report the particle detachment efficacy of MFC suspensions using concentrations (ϕ) ranging from 0.25–1 wt%. Firstly, we conduct rheological measurements to assess how varying concentration affects the fiber suspension's response to deformation. The rheological measurements shown in Fig. 2 were performed using the Anton Paar MCR302e rheometer equipped with smooth parallel plates of diameter 50 mm to determine the material characteristics of the suspension. Additionally, the normal stress measurements were performed using a smooth cone-plate of 50 mm diameter and 1-degree angle. From this, we can predict the potential cleaning efficacy based on the rheological measurements over the range of shear rates and concentrations examined. According to Fig. 2(a), the shear stress increases with increasing MFC concentration. This is intuitive since it is a common response of complex fluids as the concentrations of a deformable microstructural element is increased, thus increasing fiber–fiber and fiber–surface interactions. Also, as shown in Fig. 2(a), the shear stress generally increases with increasing shear rate for the concentrations considered. When the MFC concentration is fixed, a higher shear rate also contributes to increased fiber–fiber and fiber–surface interactions per unit time leading to a higher stress.

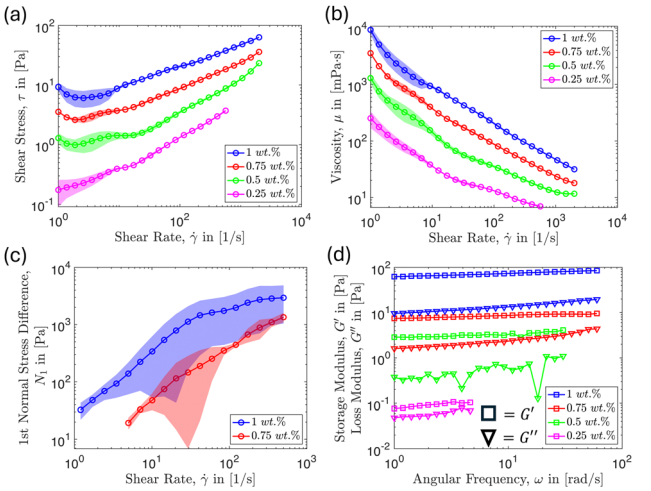

Fig. 2 Rheological measurements for different concentrations of MFC suspensions showing (a) shear stress *versus* shear rate, (b) viscosity *versus* shear rate, (c) first normal stress difference *versus* shear rate, and (d) storage and loss moduli *versus* angular frequency.

At higher MFC concentrations, fibers interlock to form an entangled fibrillar network that holds its structure when no external stresses are applied, characteristic of a yield stress fluid.[47,48] Under flow conditions, this network is broken down into flocs, which can disintegrate into individual fibers as the shear rate increases.[49,50] The flow becomes less viscous as fibers align themselves in the direction of flow, sliding against each other more easily.[51] This explains why we observe shear thinning behavior for the range of concentrations considered, as shown in Fig. 2(b). In the more concentrated regime, ($\phi \geq 1$ wt%), such observations were reported previously by Kumar *et al.*[52] Also, as shown in Fig. 2(b), as the suspension concentration decreases, fiber–fiber and fiber–wall interaction are reduced, leading to a decrease in the overall viscosity.

Moreover, according to the rheological measurements reported in Fig. 2(c), we observe larger first normal stress differences as the shear rate increases. This trend was observed to be particularly prominent for the 0.75 and 1 wt% MFC

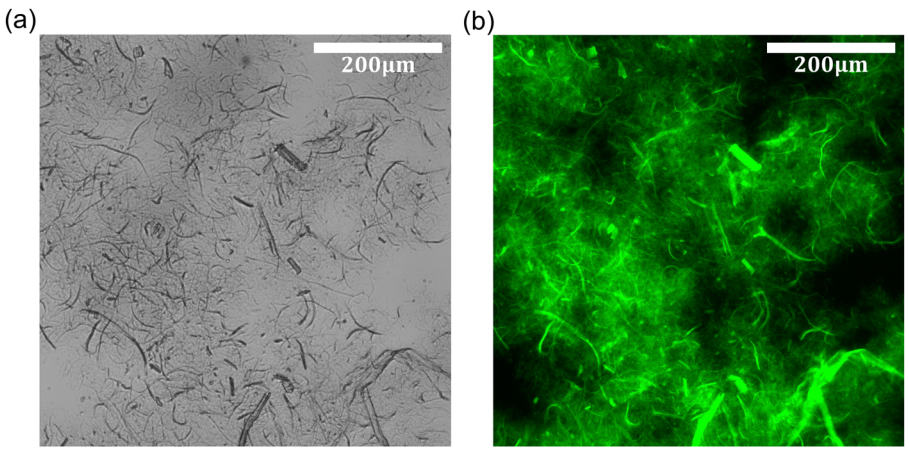

Fig. 1 Images of micro fibrillated cellulose (MFC)-water suspension at 1 wt% concentration using a 20× objective magnification in (a) bright-field microscopy and (b) fluorescence microscopy. The green represents fiber-rich regions whereas the black represents the surrounding solvent (water).

suspensions. However, we note that we did not observe measurable first normal stress differences for the 0.5 and 0.25 wt% MFC suspensions. A positive first normal stress difference implies that the stresses are directed perpendicularly toward the boundaries of the geometry. This mechanism is analogous to cleaning a surface by manually pressing and scraping off contaminants with a sponge. This implies that higher normal stresses can be a potential factor that enhances the cleaning effectiveness of the MFC suspensions. Finally, we observe that increasing fiber concentration results in higher (by orders of magnitude) storage (G') and loss (G'') moduli, as shown, respectively, in Fig. 2(d). We believe this to be potentially beneficial for cleaning applications because a higher G' implies more robust network formation: the network is less likely to break down under the same shear rate at higher concentrations, which enhances the shear stress applied to the wall. These results suggest that more efficient cleaning might be achieved by increasing the fiber concentration and shear rate.

2.2 Microfluidic device

We designed and fabricated a 1000 μm (width) × 250 μm (height) × 4 cm (length) microchannel mold on a silicon wafer using deep reactive ion etching, as sketched in Fig. 3(a). We chose this geometry to fit the experimental framework that was suitable for fluorescence microscopy and to mimic the flow-driven removal of aggregate bacteria specifically in small and narrow geometries. Then, we mixed polydimethylsiloxane (PDMS) and curing agent using a 10 : 1 ratio, degassed the mixture, poured it over the mold, and placed it into the oven to cure for approximately 2 hours. Next, we removed the PDMS elastomer and placed it into a plasma chamber together with a glass slide for plasma pre-treatment for 5 minutes. This plasma-cleaning process makes the glass surface more hydrophilic and negatively charged both for microchannel fabrication and for adhesion of positively charged particles explained in the next subsection. Finally, the patterned PDMS was joined to the glass slide to complete the channel and placed on a hot plate to complete the bonding process. The shear rates were then controlled by changing the flow rate through the channel.

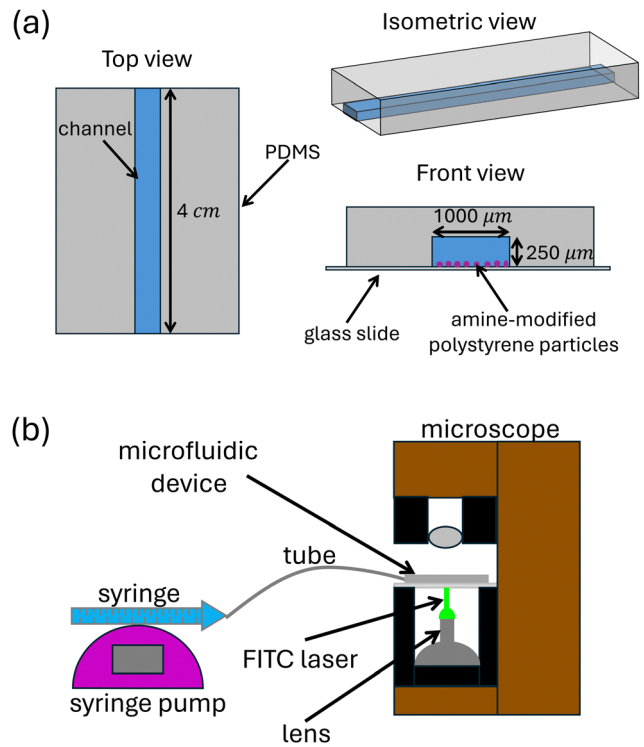

Fig. 3 (a) Diagram showing the basic design of the microchannel used in this study. (b) The general setup of the experiments.

Since the solution itself is a complex fluid we considered the possibility that the MFC could adsorb to the channel walls (PDMS). Fouling typically requires either strong interfacial interactions, *e.g.*, hydrogen bonding, electrostatic attraction, or significant surface roughness, none of which are characteristic of PDMS in contact with suspensions of microfibrillated cellulose (MFC). In particular, MFC is a highly hydrated, insoluble, hydrophilic material, while PDMS is hydrophobic with a low surface energy. Due to this contrast in surface properties, MFC should not significantly adhere to PDMS surfaces during flow. Empirical observations from our experiments also did not indicate noticeable MFC accumulation or obstruction on the PDMS surface.

2.3 Particle adhesion

Immediately after the components of the microchannel were assembled, we filled the entire channel with a solution of positively charged 2 μm diameter amine-modified polystyrene particles (Sigma Aldrich) in de-ionized water. We allowed the particles to bind to the glass for approximately 75 minutes. Plasma treatment of the glass surface induces a negative charge due to the generation of hydroxyl radicals. Thus, the positively charged particles strongly adhere to the glass slide during this time.

The strength of particle adhesion to the glass surface is described theoretically by the Derjaguin–Landau–Verwey–Overbeek (DVLO) theory,[29,53,54] which estimates the combined effects of van der Waals attraction and electrostatic forces. The DLVO theory predicts that adhesion strength will be controlled by the particle diameter, particle sphericity, surface charge of both the particle and surface, and surface energies of both materials. However, utilization of DLVO theory towards estimating particle adhesion strength is limited in practice as it requires estimation of the separation distance between the particle and surface and of the Hamaker constant.[53] In addition, electrolytic properties of the solution[55] and initial transport mechanisms of the particles towards the surface[56] will significantly influence the actual adhesion strength. Therefore, obtaining the adhesion strength of the particles was out of the scope of this study. However, we will show later in Fig. 10 that adhered *Staphylococcus aureus* respond similarly to the adhered colloids chosen in this study, under the flow of MFC suspensions.

In the present experiments, the influence of plasma treatment on the distribution and magnitude of the glass surface charge, which has a strong impact on particle adhesion strength, will depend on both environmental conditions (humidity, temperature) and chamber conditions (exact plasma striking pressure,

position of the glass slide). These factors are subject to some amount of variability across experiments. We mitigated these variations as much as reasonably possible *via* the long plasma treatment time of 5 minutes. Due to the intrinsic variability in the strength of adhesion between the particles and the glass surface, below we report averages and error bars for particle removal.

2.4 Experiment protocol

The experimental setup is sketched in Fig. 3(b). We carefully flushed the excess, non-adhered particles from the main channel with water. After this step, only the particles with a strong bond to the glass slide remained. We were careful not to introduce bubbles into our experiment as capillary forces can detach colloids from glass surfaces.[28,29] Next, we flow MFC suspensions with concentrations ranging from 0.25–1 wt% at flow rates ranging from 0.5–5 ml min^{-1}.

We control the flow rate using a syringe pump, as shown in Fig. 3(b), and subsequently estimate the wall shear rate based on the flow rate selected for a given experiment. We accomplish this by calculating the average velocity of the fluid using the relationship $U_{avg} = Q/A$, where Q is the volumetric flow rate and A is the cross-sectional area of the rectangular channel. We can then approximate the average wall shear rate by $\dot{\gamma} \approx U_{avg}/h$ where h is the height of the channel. Finally, we image particle removal with time using a fluorescence microscope, which captured 8 images per second for the exposure time; images were always taken near the center of the channel and we verified that there were no significant variations along the channel. Data was collected over an experimental duration of 2 minutes. Image post-processing and analysis were performed using ImageJ and Matlab.

3 Results and discussion

As mentioned above, the total number of adhered particles to the substrate is a difficult parameter to control as this depends on several variables. Nevertheless, we can still achieve repeatable results by keeping the experimental protocol consistent and analyzing the subsequent data appropriately by focusing on the fraction of particles removed. We find that the amine-modified particles remained strongly adhered to the glass surface for the flow of control fluids including water and a high zero-shear-rate viscosity fluid even at the larger shear rates used. For example, in Fig. 4 we visually demonstrate that the particles remain adhered under the flow of a higher viscosity water–glycerol mixture and xanthan gum polymer solutions, but are removed under the flow of 0.25 wt% MFC suspension. We note that the 0.25 wt% MFC still has trouble cleaning colloids adhered near the corner region which we will explore in detail later on.

It might have been expected that the xanthan gum solution should be effective in cleaning since, according to the results in Fig. 5, it has a higher viscosity, and storage modulus, and exerts notably larger shear and normal stresses compared to the 0.25 wt% MFC suspension. However, the xanthan gum solution is ineffective at removing the adhered colloids compared to the MFC suspension at the same shear rate. This result hints that there may be additional features apart from standard rheology that enables the MFC to detach colloids effectively.

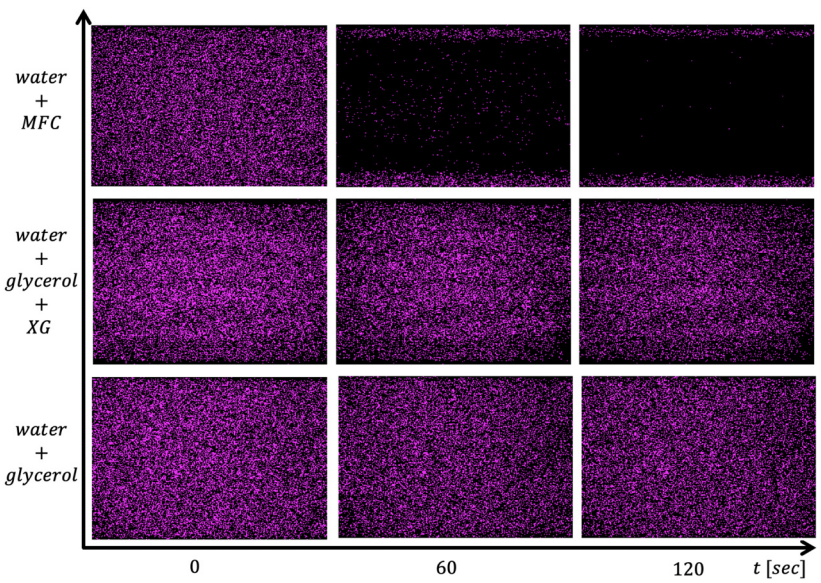

Fig. 4 Control experiments demonstrating the efficacy of a dilute MFC and water suspension compared with fluids with a higher viscosity. The top row represents time stamps of 0.25 wt% micro-fibrillated cellulose-water suspension removing adhered particles from the substrate. The middle row represents time stamps of water and glycerol (50 : 50) and xanthan gum (XG) (0.3 wt%) removing adhered particles from the substrate. The last row represents time stamps of the glycerol–water mixture (60 : 40 vol%) removing adhered particles from the substrate. These experiments were run at the same pre-selected flow rate (5 ml min^{-1}) which corresponds to an average wall shear rate of $\dot{\gamma} \approx 1300$ s^{-1}. The three images at the initial time give an indication of the typical variability in initial surface coverage. The vertical width of each frame is 1 mm in length.

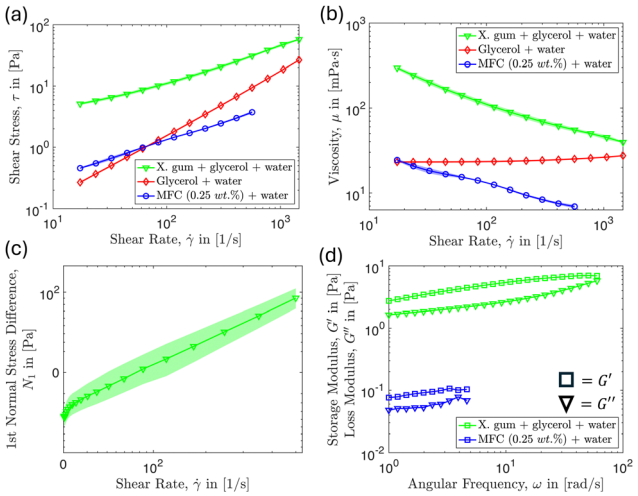

Fig. 5 Rheological measurements for control fluids, 0.3 wt% xanthan gum in glycerol and water (50 : 50 wt%) and glycerol and water solutions (60 : 40 vol%) compared to 0.25 wt% MFC in water suspension showing (a) shear stress *versus* shear rate, (b) viscosity *versus* shear rate, (c) first normal stress difference *versus* shear rate, and (d) storage and loss moduli *versus* angular frequency.

To investigate this further, we conducted tribological measurements using the 0.25 wt% MFC suspension and compared that to the glycerol–water mixture and xanthan gum polymer solution. The tribological measurements complement the rheological measurements because they highlight the frictional contribution due to the constituent microstructure interactions with the surface. In contrast, the rheological measurements discussed previously describe the behavior of the bulk fluid in response to a given rate of deformation. To obtain these tribological measurements, we use an Anton Paar MCR 302 equipped with a tribology cell with a rotating glass ball on three pins made of PDMS. The tribology cell consists of a glass ball (diameter 12.7 mm) attached to a rotating shaft (Anton Paar SP-BC12.7, length 103.75 mm). The sample holder (Anton Paar SH-BC6/T/PTD 200) is a 30 mm diameter cup-shaped component that contains the testing fluid and houses three cylindrical PDMS pins (Anton Paar SP-BC6-6/PDMS, each 6 mm in diameter). These pins are positioned equidistantly from one another and are inclined relative to the shaft. A normal force is applied to the shaft, compressing the fluid between the glass ball and the pins. Simultaneously, a torque is applied to the shaft, causing it to rotate along with the ball.

With this configuration, we measure the ratio between shear force and normal force, *i.e.*, the coefficient of friction as a function of the sliding velocity of the ball. This ratio describes how much force is required to overcome friction relative to the normal load pressing the two surfaces together. According to the results shown in Fig. 6, the tribological friction factor is higher for the 0.25 wt% MFC suspension compared to the other control fluids tested. We believe this to be representative of the local fiber interaction with the surface, which provides some explanation as to why we observe more effective cleaning with the 0.25 wt% MFC compared to the other control fluids used.

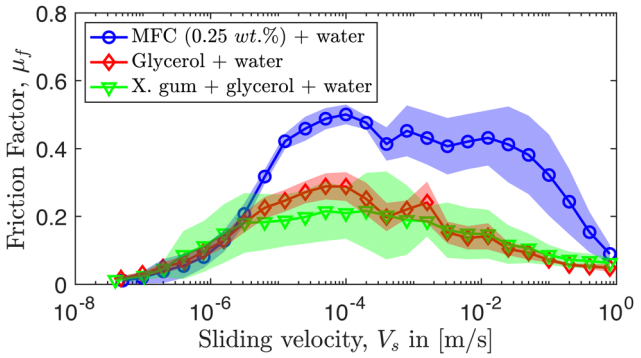

Fig. 6 Tribological friction factor as a function of sliding velocity for 0.25 wt% MFC suspension, 0.3 wt% xanthan gum in 50 : 50 wt% glycerol–water solution and 60 : 40 vol% glycerol–water mixture.

One way we can characterize cleaning effectiveness is by recording the normalized particle surface density as a function of time for different concentrations and shear rates as shown in Fig. 7, with panel (a) showing results for $\dot{\gamma} \approx 1300\ s^{-1}$ and panel (b) for $\dot{\gamma} \approx 260\ s^{-1}$ (see also Fig. 8). We define the particle surface density as the total number of adhered colloids divided by the measurement area. Then, we normalize the particle surface density of each frame by the initial particle surface density, and the results are reported in the following plots, which allow us to determine how clean the substrate is relative to the initial frame.

As reported in Fig. 2, the MFC suspension shows an overall increase in viscosity and shear stress with increasing fiber

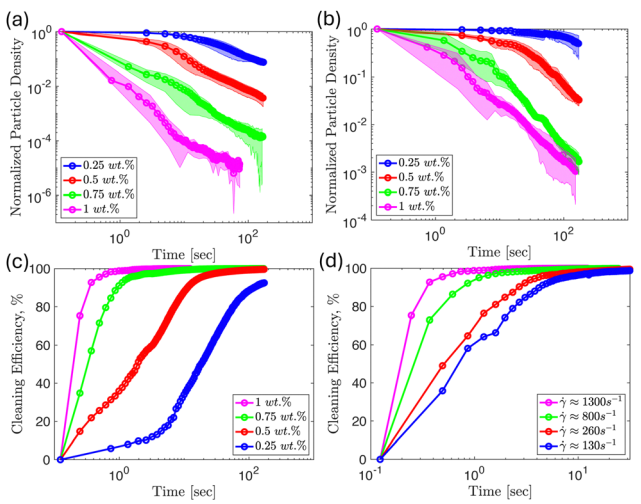

Fig. 7 MFC cleaning experiments performed at the same average shear rate respectively. The solid markers represent the averaged data whereas the shaded error bars represent the standard deviation for the respective data set. (a) Normalized particle density with time comparing the effect of different concentrations, ϕ, of micro-fibrillated cellulose suspensions at an average shear rate of $\dot{\gamma} \approx 1300\ s^{-1}$. (b) Normalized particle density with time comparing the effect of different concentrations, ϕ, of micro-fibrillated cellulose suspensions at an average shear rate of $\dot{\gamma} \approx 260\ s^{-1}$. (c) Evolution of the cleaning efficiency with time for varying concentrations of MFC suspensions. (d) Evolution of the cleaning efficiency with time for 1 wt% micro-fibrillated cellulose suspensions at varying shear rates.

concentration for the shear rates used in this study. Thus, it is expected that as we increase the MFC concentration, ϕ, we will observe faster removal of particles at the same time for a given shear rate. We confirm this intuition from the results shown in Fig. 7, which demonstrates that the particle surface coverage decreases at a faster rate when increasing the concentration of the fiber suspension for a given shear rate. We note this to be a consistent theme at every flow rate (shear rate) studied. We interpret this result as occurring because a higher MFC concentration corresponds to greater wall stress and fiber-particle interactions leading to faster removal.

Also, we were interested in measuring the cleaning efficiency of each suspension, which we define as the fraction of the initial number of colloids removed, here reported as a percentage. We define the cleaning efficiency as:

$$\eta_{CE} = \frac{\text{initial \# of colloids} - \text{\# of colloids removed}}{\text{initial \# of colloids}} \times 100 \quad (1)$$

such that 0% indicates no removal and 100% is complete removal. The results are displayed in Fig. 7(c). Unsurprisingly, the higher MFC concentrations enable higher cleaning efficiency at shorter times. For ϕ = 1 wt% only a few seconds are needed to remove nearly 100% of the initial number of adhered particles for the geometry and size of the microchannel and the shear rate used. In contrast, we show that the efficiency of the 1 wt% MFC suspension is reduced if we flow at lower shear rates, as shown in Fig. 7(d). Additionally, we find that more dilute suspensions, *e.g.*, 0.5 wt%, can be just as efficient at longer times. We believe that the increasing robustness of the fibrillar network with increasing concentration contributes to faster removal at 0.75 and 1 wt% compared to lower concentrations. However, network formation is not required for effective cleaning as the more dilute concentrations that have limited fiber-to-fiber interactions, *e.g.*, 0.25 wt%, eventually remove more than 80% of particles as shown in Fig. 7(c). It was reported by Walker *et al.*[38] that water was only effective in removing weakly adhered colloids, which is congruent with our control experiments discussed previously. Therefore, we hypothesize that the bulk solvent (water) had a limited effect on removing particles and detachment was largely due to fiber floc-particle interactions, which increase with fiber concentration.

We expect the corners of the channels to be hindrances to cleaning as noted earlier from the control experiments shown in Fig. 4. We measured the normalized particle surface density as a function of distance across the width of a channel, with zero corresponding to the position of a corner and 0.5 corresponding to the middle of the channel. The results are shown in Fig. 8 for different MFC concentrations, where we observe that all of the fiber suspensions will eventually completely clean particles from the center of the channel (initial time shown in blue, final time in pink). However, as suspensions become more dilute, particle detachment in the neighborhood of the corners poses a challenge even at longer times. From the results shown in Fig. 8(a), the 1 wt% suspension removes the majority of the particles in the main channel in less than half a second. However, the particles near the corners remain relatively

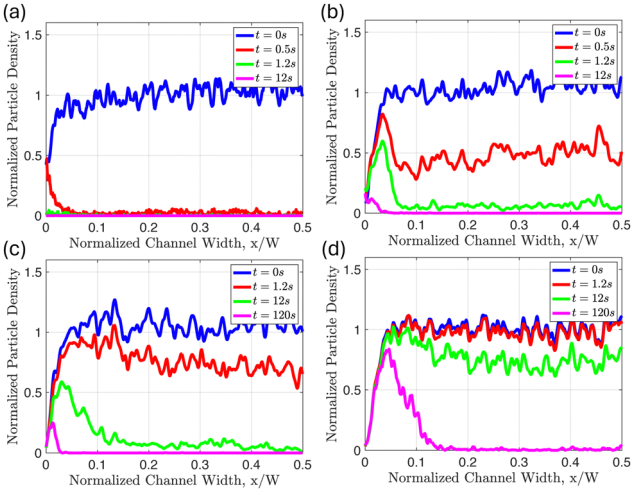

Fig. 8 Results for the particle density profile as a function of channel width at different times for (a) ϕ = 1 wt%, (b) ϕ = 0.75 wt%, (c) ϕ = 0.5 wt%, and (d) ϕ = 0.25 wt%. All experiments shown were performed at a shear rate $\dot{\gamma} \approx 1300\ s^{-1}$.

untouched. In this particular case, the flow requires an additional 11 seconds before the 1 wt% fiber suspension removes the particles near the corners.

For the 0.75 wt% suspension shown in Fig. 8(b), roughly half of the initial particles are removed across the width of the channel after half a second. After 12 seconds, particles are completely removed from the center of the channel, with some particles remaining near the corners. We note that the normalized particle surface density is reduced near the corners at longer times for the 0.75 wt% concentration. Further, diluting the suspension to a concentration of 0.5 wt% results in needing about 10 times the time to achieve a similar surface density profile across the width of the channel compared to the 0.75 wt% results. The pink curve in Fig. 8(c) shows that there is still about 25% of the initial surface density of particles accumulated near the corners at the end of the experiment duration. Lastly, for the 0.25 wt% suspension results displayed in Fig. 8(d), the overall particle surface density in the channel, and the region of particle accumulation near the edges are both increased compared to the 0.5 wt% results over the same period. At the end of the experiment, the pink curve in this panel shows that most of the particles near the center of the channel are removed. However, the accumulation of particles near the corners in Fig. 8(d) is only reduced slightly relative to the initial particle density. Therefore, the results suggest that higher concentrations of MFC are more effective in detaching colloids near the corner regions. We note that dilute MFC suspensions can still be effective in detaching colloids in systems where corners are not present.

The reduction in cleaning effectiveness as we approach the corner may be because of the lower local velocity, and so the local shear rate of the fibers in this region is lower than near the center of the channel. This leads to a reduced rate of fiber-particle interactions near the corners. Additionally, previous studies have indicated that the fibers migrate away from the

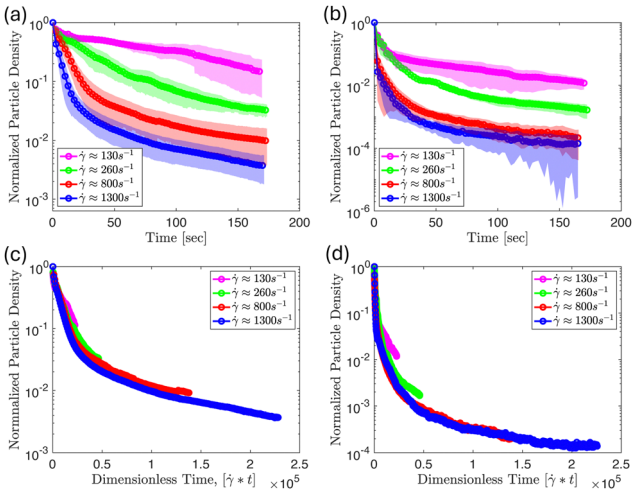

Fig. 9 Results for colloidal detachment using a fixed concentration of MFC suspension while varying the average shear rate. The solid markers represent the average of 5 data sets whereas the shaded error bars represent the standard deviation for the respective data set. (a) Normalized particle surface density removal using 0.75 wt% for different shear rates. (b) Normalized particle surface density removal using 0.5 wt% for different shear rates. (c) Data collapse for 0.75 wt% MFC suspension when time is normalized with the corresponding shear rate for each experiment. (d) Data collapse for 0.5 wt% MFC suspension when time is normalized with the corresponding shear rate for each experiment.

wall and accumulate near the center of the channel under flow conditions.[52,57,58] This results in a decrease in fiber concentration near the corners, which becomes more apparent for more dilute suspensions. Thus, reduced fiber velocity, and possibly concentration, near the corners make cleaning less effective in this region. Since the results presented in Fig. 8 hint at cleaning effectiveness being affected by the local shear rate across channel width, this prompted us to conduct experiments varying the flow rate (and so the shear rate) while keeping the MFC concentration fixed. The results in Fig. 9(a and b) suggest that when the fiber concentration is fixed, increasing the shear rate increases the rate of colloidal detachment across the entire channel. This result is consistent among all the concentrations we considered. We elucidate the generality of this shear rate effect by making the x-axis dimensionless, normalizing time with the respective shear rate. It is evident from the results in Fig. 9(c and d) that the data collapses when the normalized particle surface density for each shear rate is plotted against dimensionless time. This shows that the shear rate is the main variable affecting the particle removal rate when the concentration of fibers is fixed.

As one indication of an application of these ideas one can also consider the removal of bacterial aggregates from surfaces. We report preliminary experiments using MFC suspensions to remove *Staphylococcus aureus* bacteria from the glass surface in the same channel configuration as performed with the amine-modified particles. In Fig. 10, we compare the removal of amine-modified particles with the removal of *Staphylococcus aureus* under the flow of 0.5 wt% MFC suspension. For the experiments performed the bacteria seem to be removed more easily than the amine-modified particles, as shown in Fig. 10(b). In general, the reduction in bacteria surface density for *Staphylococcus aureus* has a similar trend to the particles.

To summarize, we sought to connect rheology to the cleaning efficiency of micro-fibrillated cellulose suspensions. We have observed the best cleaning from the 0.75 and 1 wt% MFC suspensions compared to the other fluid systems introduced above. The MFC suspensions have a notably higher G' which we believe indicates a more robust fibrillar network that enhances shear stresses. We also measured a larger first

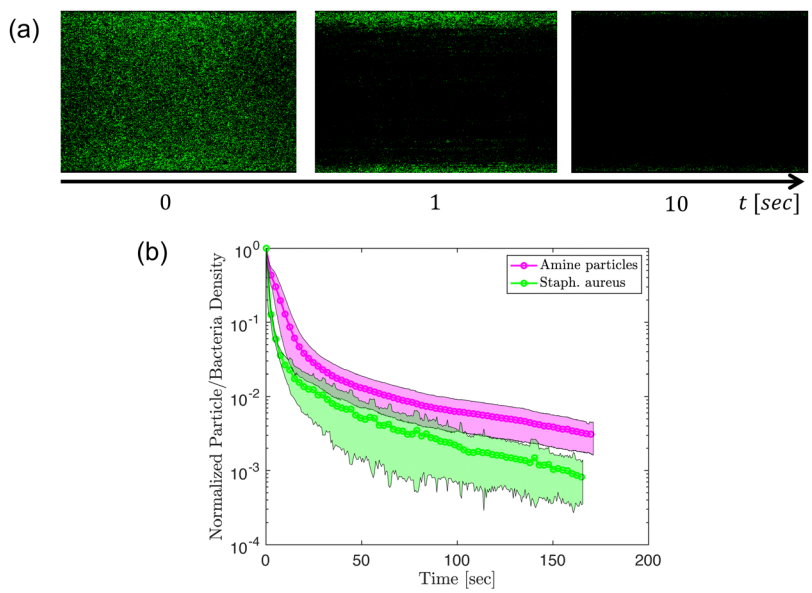

Fig. 10 (a) Visualization of 0.5 wt% MFC suspension removing *Staphylococcus aureus* bacteria from substrate. The vertical width of each frame is 1 mm in length. (b) Plot showing the reduction in the density of *Staphylococcus aureus* compared to the removal of amine-modified particles as a function of time under the flow of 0.5 wt% MFC suspension.

normal stress difference (N_1) for the 0.75 and 1 wt% MFCs, which may contribute to effective cleaning as a higher N_1 results in enhanced fiber-particle interactions as the fluid presses against the boundaries, including the corners, to a greater extent compared to more dilute MFC suspensions. However, we recognize that this argument is insufficient to explain the cleaning efficacy of lower concentrations such as the 0.25 wt% MFC. We noted earlier that the 0.25 wt% MFC suspension is more effective in detaching adhered colloids despite having a lower viscosity, storage modulus, and shear and normal stresses than xanthan gum and glycerol mixtures, which are not as effective in cleaning. Here we believe that the tribological friction measurements of the MFC suspension, which are higher than those of the control fluids, may rationalize these observations. Future research efforts will explore the characterization of the frictional effects experimentally to explore this hypothesis. Nevertheless, we believe that the high shear stresses, normal stresses, storage modulus, and fibrous microstructure are all complementary characteristics that enable the micro-fibrillated cellulose suspensions to be highly effective in cleaning.

Conclusions

In summary, we have demonstrated the cleaning efficacy of different concentrations of MFC suspensions for varying shear rates, highlighting the potential of these newly explored materials for various surface cleaning applications. The results from our experiments show that flowing higher concentrations at higher shear rates leads to more efficient cleaning, which is consistent with our intuition based on the material's rheology (higher shear and normal stresses at higher shear rates). However, we found that standard rheological measurements were not sufficient to fully describe the cleaning efficacy of the MFC. Indeed, the tribological results suggest that the wall friction due to the material's microstructure plays a vital role. We observed that the dilute concentrations of MFC suspensions were less effective at removing particles near the corners. Therefore, we recommend choosing higher concentrations for rectangular geometries so that fibers can reach particles near the corner region.

By keeping concentration fixed and varying the flow rates we were able to show the decreasing cleaning effectiveness of the respective concentration as the average applied shear rate was decreased. By normalizing time with the shear rate we documented that for a fixed concentration the shear rate is the main parameter affecting the removal rate of adhered particles from the substrate. The present study implies that increasing the frequency of particle-fiber interactions at the wall, whether by increasing the shear rate and/or fiber concentration is essential for effective contaminant removal. Further efforts could focus on extending this work to other kinds of contaminants such as bacteria and biofilms in more complex geometries.

Data availability

The datasets generated and/or analysed during the current study are available in the Github repository named "MFCcleaningdata" accessed *via* **https://github.com/mmlouis/MFCcleaning**
datahere.

Conflicts of interest

The authors declare the following financial interests/personal relationships which may be considered as potential competing interests: Mohamed E. Labib, Antonio Perazzo, Christopher A. Kuchar are employees of NovaFlux, Inc. and consultants to Protegera, Inc., which are two companies involved in the development and commercialization of microfibrillated cellulose-based technologies.

Acknowledgements

The Princeton team thanks Novaflux and Princeton University for support of this research *via* Princeton's Innovation Fund for Industrial Collaborations. The authors also thank J. Hwang for his guidance in conducting some of the rheological measurements. S. McBride was partially supported by the Princeton Presidential Postdoctoral Fellows Program. We thank the Princeton Materials Research Science and Engineering Center for partial support of this research (MRSEC, DMR-2011750).

Notes and references

1 M. B. Ranade, *Aerosol Sci. Technol.*, 1987, **7**, 161–176.
2 J. Visser, *Part. Sci. Technol.*, 1995, **13**, 169–196.
3 M. Schoenitz, L. Grundemann, W. Augustin and S. Scholl, *Chem. Commun.*, 2015, **51**, 8213–8228.
4 A. Deshpande, G. W. G. Smith and A. J. Smith, *J. Hosp. Infect.*, 2015, **90**, 179–185.
5 Y. Fang, Z. Shen, L. Li, Y. Cao, L. Y. Gu, Q. Gu, X. Q. Zhong, C. H. Yu and Y. M. Li, *World J. Gastroenterol.*, 2010, **16**, 1019–1024.
6 W. Ren-Pei, X. Hui-Jun, Q. Ke, W. Dong, N. Xing and L. Zhao-Shen, *Am. J. Infect. Control*, 2014, **42**, 1203–1206.
7 H. B. Allen, N. D. Vaze, C. Choi, T. Hailu, B. H. Tulbert, C. A. Cusack and S. G. Joshi, *JAMA Dermatol.*, 2014, **150**, 260–265.
8 M. Brandwein, D. Steinberg and S. Meshner, *NPJ Biofilms Microbiomes*, 2016, **2**, 3.
9 M. M. Severn and A. R. Horswill, *Nat. Rev. Microbiol.*, 2023, **21**, 97–111.
10 M. O. Schmid, O. P. Balmelli and U. P. Saxer, *J. Clin. Periodontol.*, 1976, **3**, 157–165.
11 S. Sälzer, D. E. Slot, F. A. Van Der Weijden and C. E. Dörfer, *J. Clin. Periodontol.*, 2015, **42**, S92–S105.
12 F. Zhang, A. A. Busnaina, A. M. Fury and S.-Q. Wang, *J. Electron. Mater.*, 2000, **29**, 199–204.
13 D. W. Cooper, *Aerosol Sci. Technol.*, 1986, **5**, 287–299.
14 A. Busnaina, J. Taylor and I. Kashkoush, *J. Adhes. Sci. Technol.*, 1993, **7**, 441–455.

15 M. Toofan and J. Toofan, in *Developments in Surface Contamination and Cleaning*, ed. R. Kohli and K. Mittal, William Andrew Publishing, Oxford, 2015, pp. 185–212.
16 K. Xu, R. Vos, G. Vereecke, G. Doumen, W. Fyen, W. P. Mertens, M. M. Heyns, C. Vinckier and J. Fransaer, *J. Vac. Sci. Technol., B: Microelectron. Nanometer Struct.--Process., Meas., Phenom.*, 2004, 2844–2852.
17 Y. Huang, D. Guo, X. Lu and J. Luo, *Appl. Surf. Sci.*, 2011, **257**, 3055–3062.
18 G. Kumar and S. Beaudoin, *J. Electrochem. Soc.*, 2006, **153**, G175.
19 R. Mastrangelo, D. Chelazzi, G. Poggi and P. Baglioni, *Proc. Natl. Acad. Sci. U. S. A.*, 2020, **117**, 7011–7020.
20 B. D. Napoli, S. Franco, L. Severini, M. Tumiati, E. Buratti, M. Titubante, V. Nigro, N. Gnan, L. Micheli, B. Ruzicka, C. Mazzuca, R. Angelini, M. Missori and E. Zaccarelli, *ACS Appl. Polym. Mater.*, 2020, **2**, 2791–2801.
21 C. Mazzuca, L. Micheli, M. Carbone, F. Basoli, E. Cervelli, S. Iannuccelli, S. Sotgiu and A. Palleschi, *J. Colloid Interface Sci.*, 2014, **416**, 205–211.
22 R. Amin, L. Li and S. Tasoglu, *Talanta*, 2019, **192**, 455–462.
23 Q. Tu, J.-C. Wang, Y. Zhang, R. Liu, W. Liu, L. Ren, S. Shen, J. Xu, L. Zhao and J. Wang, *Rev. Anal. Chem.*, 2012, **31**, 177–192.
24 K. Georgieva, D. J. Dijkstra, H. Fricke and N. Willenbacher, *J. Colloid Interface Sci.*, 2010, **352**, 265–277.
25 A. J. Volker Heinzel and H. Sauter, *Heat Transfer Eng.*, 2007, **28**, 222–229.
26 A. M. D. Wan, D. Devadas and E. W. K. Young, *Sens. Actuators, B*, 2017, **253**, 738–744.
27 C. Gómez-Suárez, H. C. Van Der Mei and H. J. Busscher, *J. Adhes. Sci. Technol.*, 2000, **14**, 1527–1537.
28 S. Khodaparast, M. K. Kim, J. E. Silpe and H. A. Stone, *Environ. Sci. Technol.*, 2017, **51**, 1340–1347.
29 P. Sharma, M. Flury and J. Zhou, *J. Colloid Interface Sci.*, 2008, **326**, 143–150.
30 S. Aramrak, M. Flury and J. B. Harsh, *Langmuir*, 2011, **27**, 9985–9993.
31 C. Gómez-Suárez, H. J. Busscher and H. C. Van Der Mei, *Appl. Environ. Microbiol.*, 2001, **67**, 2531–2537.
32 V. Lazouskaya, L. P. Wang, D. Or, G. Wang, J. L. Caplan and Y. Jin, *J. Colloid Interface Sci.*, 2013, **406**, 44–50.
33 Y. Seo, J. Leong, J. D. Park, Y. T. Hong, S. H. Chu, C. Park, D. H. Kim, Y. H. Deng, V. Dushnov, J. Soh, S. Rogers, Y. Y. Yang and H. Kong, *ACS Appl. Mater. Interfaces*, 2018, **10**, 35685–35692.
34 R. Zhou, R. Zhou, P. Wang, B. Luan, X. Zhang, Z. Fang, Y. Xian, X. Lu, K. K. Ostrikov and K. Bazaka, *ACS Appl. Mater. Interfaces*, 2019, **11**, 20660–20669.
35 W. Kim, T. H. Kim, J. Choi and H. Y. Kim, *Appl. Phys. Lett.*, 2009, **94**, 8.
36 V. A. Andreev, E. M. Freer, J. M. de Larios, J. M. Prausnitz and C. J. Radke, *J. Electrochem. Soc.*, 2011, **158**, H55.
37 H. Hirano, K. Sato, T. Osaka, H. Kuniyasu and T. Hattori, *Electrochem. Solid-State Lett.*, 2006, **9**, 2.
38 T. W. Walker, T. T. Hsu, S. Fitzgibbon, C. W. Frank, D. S. L. Mui, J. Zhu, A. Mendiratta and G. G. Fuller, *J. Rheol.*, 2014, **58**, 63–88.
39 S. Yiantsios and A. Karabelas, *J. Colloid Interface Sci.*, 1995, **176**, 74–85.
40 J. Noordmans, P. J. Wit, H. C. Van Der Mei and H. J. Busscher, *J. Adhes. Sci. Technol.*, 1997, **11**, 957–969.
41 L. Walsh, *Aust. Dent. Pract.*, 2024, **July/August**, 80–86.
42 J. R. Landel and D. I. Wilson, *Annu. Rev. Fluid Mech.*, 2021, **53**, 147–171.
43 M. E. Labib, A. Perazzo, J. L. Manganaro, Y. Tabani, C. J. Durham, B. R. Schemehorn, H. C. McClure and L. J. Walsh, *J. Dent.*, 2024, **146**, 105038.
44 M. E. Labib, A. Perazzo, J. Manganaro, Y. Tabani, K. R. Milleman, J. L. Milleman and L. J. Walsh, *Dent. J.*, 2024, **12**, 1.
45 I. Siró and D. Plackett, *Cellulose*, 2010, **17**, 459–494.
46 M. Babi, A. Fatona, X. Li, C. Cerson, V. M. Jarvis, T. Abitbol and J. M. Moran-Mirabal, *Biomacromolecules*, 2022, **23**, 1981–1994.
47 T. Turpeinen, A. Jäsberg, S. Haavisto, J. Liukkonen, J. Salmela and A. I. Koponen, *Cellulose*, 2020, **27**, 141–156.
48 S. Mohan, J. Jose, A. Kuijk, S. J. Veen, A. Van Blaaderen and K. P. Velikov, *ACS Omega*, 2017, **2**, 5019–5024.
49 E. G. Facchine, R. J. Spontak, O. J. Rojas and S. A. Khan, *Biomacromolecules*, 2020, **21**, 3561–3570.
50 J. Lauri, S. Haavisto, J. Salmela, A. Miettinen, T. Fabritius and A. I. Koponen, *Cellulose*, 2021, **28**, 3373–3387.
51 M. C. Li, Q. Wu, R. J. Moon, M. A. Hubbe and M. J. Bortner, *Adv. Mater.*, 2021, **33**, 2006052.
52 V. Kumar, B. Nazari, D. Bousfield and M. Toivakka, *Appl. Rheol.*, 2016, **26**, 4.
53 M. Corn, *J. Air Pollut. Control Assoc.*, 1961, **11**, 523–528.
54 Z. Adamczyk and P. Weroński, *Adv. Colloid Interface Sci.*, 1999, **83**, 137–226.
55 Z. Adamczyk and P. Warszyński, *Adv. Colloid Interface Sci.*, 1996, **63**, 41–149.
56 Z. Adamczyk, B. Siwek and M. Zembala, *Colloids Surf., A*, 1993, **76**, 115–124.
57 S. Haavisto, J. Liukkonen, A. Jäsberg, A. Koponen, M. Lille and J. Salmela, *Laboratory-Scale Pipe Rheometry: A Study of a Microfibrillated Cellulose Suspension*, 2011.
58 T. Saarinen, S. Haavisto, A. Sorvari, J. Salmela and J. Seppälä, *Cellulose*, 2014, **21**, 1261–1275.